



Condensed Matter and Interphases

Kondensirovannye Sredy i Mezhfaznye Granitsy
<https://journals.vsu.ru/kcmf/>

Original articles

Research article

<https://doi.org/10.17308/kcmf.2024.26/11937>

X-ray luminescence of $\text{Sr}_{0.925-x}\text{Ba}_x\text{Eu}_{0.075}\text{F}_{2.075}$ nanopowders

Yu. A. Ermakova, P. P. Fedorov, V. V. Voronov, S. Kh. Batygov, S. V. Kuznetsov✉

Prokhorov General Physics Institute of the Russian Academy of Sciences,
38, Vavilova str., Moscow 119991, Russian Federation

Abstract

We synthesized powders of single-phase solid solutions $\text{Sr}_{0.925-x}\text{Ba}_x\text{Eu}_{0.075}\text{F}_{2.075}$ ($x = 0.00, 0.20, 0.25, 0.30, 0.35$ and 0.40) by a precipitation technique from nitrate aqueous solutions. The lattice parameters increase linearly as the barium content increases. We recorded a significant increase in the X-ray luminescence intensity of europium at increasing barium content. Upon increasing barium content, the intensity of the luminescence of strong $^5\text{D}_0 \rightarrow ^7\text{F}_1$ band increases exponentially, and we observed blue and red shifts in the position of the europium luminescence bands for $^5\text{D}_0 \rightarrow ^7\text{F}_1$ and $^5\text{D}_0 \rightarrow ^7\text{F}_4$, respectively.

Keywords: Strontium fluoride, Barium fluoride, Europium, X-ray luminescence

Funding: The study was supported by Russian Science Foundation grant No. 22-13-00401, <https://rscf.ru/en/project/22-13-00401/>.

For citation: Ermakova Yu. A., Fedorov P. P., Voronov V. V., Batygov S. Kh., Kuznetsov S. V. X-ray luminescence of $\text{Sr}_{0.925-x}\text{Ba}_x\text{Eu}_{0.075}\text{F}_{2.075}$ nanopowders. *Condensed Matter and Interphases*. 2024;26(2): 247–252. <https://doi.org/10.17308/kcmf.2024.26/11937>

Для цитирования: Ермакова Ю. А., Федоров П. П., Воронов В. В., Батыгов С. Х., Кузнецов С. В. Рентгенолюминесценция нанопорошков $\text{Sr}_{0.925-x}\text{Ba}_x\text{Eu}_{0.075}\text{F}_{2.075}$. *Конденсированные среды и межфазные границы*. 2024;26(2): 247–252. <https://doi.org/10.17308/kcmf.2024.26/11937>

✉ Sergey V. Kuznetsov e-mail: kouznetsovsv@gmail.com

© Ermakova Yu. A., Fedorov P. P., Voronov V. V., Batygov S. Kh., Kuznetsov S. V., 2024



The content is available under Creative Commons Attribution 4.0 License.

1. Introduction

A new direction in diamond photonics is the incorporation of rare-earth elements into the diamond crystal lattice in such a way as to form a luminescent center with luminescence bands of the incorporated ion. To date, there are two main technological approaches. The first one is the use of precursors (both inorganic and organic) obtained by chemical vapor deposition (CVD) or high pressure-high temperature (HPHT) methods [1–5]. The second method is the incorporation of nanoparticles of the target composition and their physical encapsulation inside the diamond using the CVD method [6]. The second approach shows the most intense luminescence. This is due to the fact that the incorporated target substances have rigorously selected functional compositions. Europium is used as a luminescent ion in most of the studies, since it is a probe element that allows both to detect the local environment and control its change, and to detect the reduction processes due to the possibility of the $\text{Eu}^{3+} \rightarrow \text{Eu}^{2+}$ transition. So far, Eu_2O_3 [2], CeF_3 [7], HoF_3 [8], EuF_3 [9], and $\beta\text{-NaGdF}_4\text{:Eu}$ [10] have been successfully incorporated to diamond. To interpret the luminescence response reliably, it is necessary to achieve the highest luminescence intensity from the designed composite material. For this purpose, it is necessary to select a luminophore composition that does not exhibit concentration quenching or polymorphic transformations at the high temperatures of the nanoparticle incorporation process. Fluorides of alkaline-earth elements [11, 12] are effective thermally stable luminescent matrices with a wide range of doping with rare earth elements. They do not exhibit polymorphic transformations up to the melting point. To prepare fluoride powders, various synthesis methods are used, such as mechanochemistry, combustion, fluoroacetate decomposition, solvothermal and hydrothermal techniques, as well as co-precipitation from aqueous solutions, which allows obtaining large batches of powders [13–17]. In the series of $\text{CaF}_2 \rightarrow \text{SrF}_2 \rightarrow \text{BaF}_2$ difluorides having the same structural type, the energy of matrix phonons decreases [18]. This may lead to an increase in the luminescence light output by preventing multiphonon relaxation. Solid solutions based

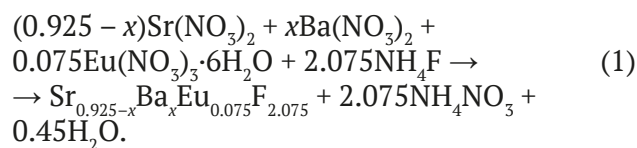
on barium fluoride and rare earth elements are not synthesized by solution-based techniques. This is why the main attention is focused on the strontium fluoride matrix. In the literature, there is a large amount of data on the photoluminescent characteristics of europium [19–24]. Drobysheva et al. [25] determined that the optimal concentrations for $\text{SrF}_2\text{:Eu}$ solid solutions are 7.5 and 15.0 mol. % Eu when excited by X-ray tubes with tungsten and silver anodes, respectively. An increase in the luminescence intensity can be achieved by reducing the phonon energy of the matrix through replacing the matrix cation with a heavier one. In the case of the strontium fluoride matrix, it is barium fluoride.

The aim of the study was to test the approach of increasing the luminescence intensity of europium by making the matrix heavier in the concentration series of $\text{Sr}_{1-x}\text{Ba}_x\text{F}_2\text{:Eu}$ (7.5 mol. %) at a variable barium content.

2. Experimental

Initial reagents. The initial substances were: $\text{Sr}(\text{NO}_3)_2$ (99.99 %, Lanhit), $\text{Ba}(\text{NO}_3)_2$ (99.99 %, Vekton), $\text{Eu}(\text{NO}_3)_3 \cdot 6\text{H}_2\text{O}$ (99.99 %, Lanhit), NH_4F (chemically pure, Lanhit), and bidistilled water of our own production. We did not further purify the reagents.

Synthesis methodology. By precipitation from aqueous solutions, we synthesized a concentration series of $\text{Sr}_{0.925-x}\text{Ba}_x\text{Eu}_{0.075}\text{F}_{2.075}$ solid solution powders ($x = 0.00, 0.20, 0.25, 0.30, 0.35$ and 0.40) by equation (1).



The powders were synthesized by the dropwise addition of nitrate solution ($C = 0.08$ M) into a polypropylene reactor with ammonium fluoride solution (0.16 M, 7% excess). The resulting suspension was stirred using a magnetic mixer for 2 hours. After sedimentation of the precipitate, the mother solution was decanted, and the precipitate was washed with a 0.5 % ammonium fluoride solution. The efficiency of nitrate ion washing out was controlled by qualitative reaction with diphenylamine. The washed precipitate was air-

dried at 45 °C. High-temperature treatment was carried out in platinum crucibles at 600 °C for 1 hour at a heating rate of 10 °/min.

X-ray diffraction (XRD) was performed on a Bruker D8 Advance diffractometer with $\text{CuK}\alpha$ radiation ($\lambda = 1.5406 \text{ \AA}$). The lattice parameters (a) and coherent scattering regions (D) were calculated in TOPAS ($R_{wp} < 7$).

The X-ray luminescence spectra of single-phase powders were recorded at room temperature on an FSD-10 minispectrometer (JSC *Optofiber*) in the range of 200–1100 nm with a resolution of 1 nm under excitation by an X-ray tube with a chromium anode operating at 30 kV and 30 mA.

3. Results of synthesis

of $\text{Sr}_{0.925-x}\text{Ba}_x\text{Eu}_{0.075}\text{F}_{2.075}$ solid solutions

The X-ray diffraction patterns of the $\text{Sr}_{0.925-x}\text{Ba}_x\text{Eu}_{0.075}\text{F}_{2.075}$ solid solution samples with the molar fraction of barium of 0.00, 0.20, 0.25, 0.30, 0.35, and 0.40, air-dried at 45 °C and heat-treated at 600 °C are shown in Fig. 1a. Annealing at 600 °C is necessary to dehydrate the powders and increase the luminescence intensity by removing the hydroxyl ion that quenches the luminescence.

The X-ray diffraction analysis showed that the synthesis of the solid solutions resulted in the formation of single-phase powders of fluorite structure (JCPDS# 06-0262, $a = 5.800 \text{ \AA}$ for SrF_2), but with a shifted position of X-ray reflections. This indicates a change in lattice parameters proportional to the amount of BaF_2 doping component. The process is followed by the incorporation of additional fluorine ions for electrostatic compensation and the formation of clusters such as $\text{REE}_6\text{F}_{36}$ (REE are rare-earth elements). The results of calculating the lattice parameters are summarized in Table 1 and presented in Fig. 2. The X-ray reflections are highly broadened, indicating the synthesis of nanoscale substances (Table 1). The size of the coherent scattering regions D was about 16–18 nm. The synthesized powders were heat-treated at 600 °C in order to dehydrate them. The process temperature was chosen based on literature review. The X-ray diffraction patterns of the heat-treated samples are provided in Fig. 1b. Comparing the X-ray diffraction patterns of the samples, we revealed a narrowing of the X-ray reflections. This indicates an increase in the coherent scattering region by several times and an increase in the

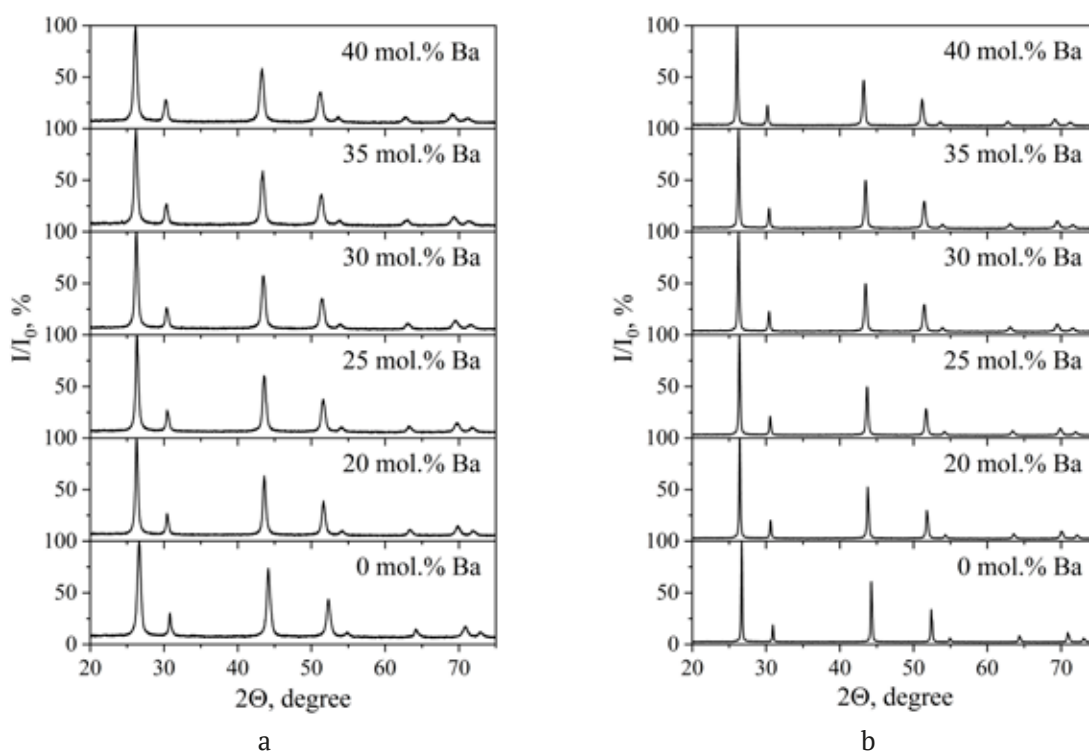


Fig. 1. X-ray diffraction patterns of $\text{Sr}_{0.925-x}\text{Ba}_x\text{Eu}_{0.075}\text{F}_{2.075}$ solid solutions: a – after drying in air at temperature of 45 °C, b – after heat treatment at temperature of 600 °C

Table 1. Lattice parameters of $\text{Sr}_{0.925-x}\text{Ba}_x\text{Eu}_{0.075}\text{F}_{2.075}$ solid solutions

Sample composition	Heat treatment			
	45 °C		600 °C	
	<i>a</i> , Å	D, nm	<i>a</i> , Å	D, nm
$\text{Sr}_{0.925}\text{Eu}_{0.075}\text{F}_{2.075}$	5.800(1)	14(1)	5.793(1)	77(1)
$\text{Sr}_{0.725}\text{Ba}_{0.200}\text{Eu}_{0.075}\text{F}_{2.075}$	5.869(1)	18(1)	5.859(1)	103(4)
$\text{Sr}_{0.675}\text{Ba}_{0.250}\text{Eu}_{0.075}\text{F}_{2.075}$	5.885(3)	15(1)	5.875(1)	65(5)
$\text{Sr}_{0.625}\text{Ba}_{0.300}\text{Eu}_{0.075}\text{F}_{2.075}$	5.901(1)	17(1)	5.889(1)	89(5)
$\text{Sr}_{0.575}\text{Ba}_{0.350}\text{Eu}_{0.075}\text{F}_{2.075}$	5.915(1)	16(1)	5.905(1)	70(8)
$\text{Sr}_{0.525}\text{Ba}_{0.400}\text{Eu}_{0.075}\text{F}_{2.075}$	5.930(1)	16(1)	5.921(1)	100(6)

particle size, which is confirmed by the calculation (Table 1). The calculated lattice parameters are described by the linear equation $a = 5.794 + 0.003x$ ($x = \text{mol.}\% \text{BaF}_2$) ($R^2 = 0.999$) (Fig. 2). They are slightly lower, which confirms the dehydration process during heat treatment (Table 1).

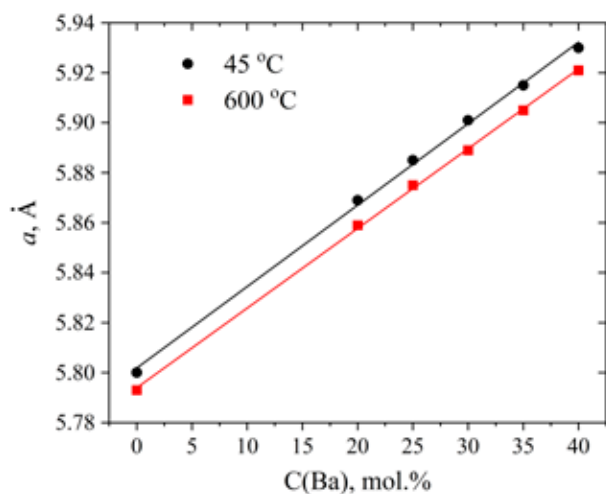
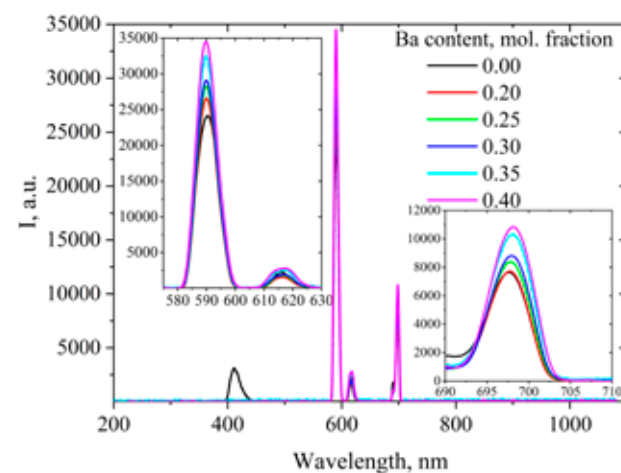
The X-ray luminescence spectra of single-phase solid solution samples of $\text{Sr}_{0.925-x}\text{Ba}_x\text{Eu}_{0.075}\text{F}_{2.075}$ after heat treatment at 600 °C are shown in Fig. 3. The luminescence spectra show trivalent europium luminescence bands with maxima at 590 nm, 617 nm, and 698 nm, corresponding to the $^5\text{D}_0 \rightarrow ^7\text{F}_i$ transitions ($i = 1, 2, 4$). The barium-free composition has a band of divalent europium.

Analysis of the X-ray luminescence spectra revealed that the intensity of the europium luminescence bands increases with increasing barium content ($^5\text{D}_0 \rightarrow ^7\text{F}_1$ with a maximum around 590 nm and $^5\text{D}_0 \rightarrow ^7\text{F}_4$ with a maximum around 698 nm). The increase in the intensity of the $^5\text{D}_0 \rightarrow ^7\text{F}_2$ band is less significant. This band

is complex and consists of several components, whose intensity varies as the barium content increases. When the barium content increases, the $^5\text{D}_0 \rightarrow ^7\text{F}_1$ luminescence band undergoes a blue shift, and $^5\text{D}_0 \rightarrow ^7\text{F}_4$ undergoes a red shift of the maximum. The intensity of the $^5\text{D}_0 \rightarrow ^7\text{F}_1$ luminescence band increases with increasing barium content (Fig. 4) according to the exponential function $I = 24445 + 230e^{(10x)}$ with approximation reliability criterion ($R^2 = 0.99227$).

4. Conclusions

Powders of single-phase solid solutions of $\text{Sr}_{0.925-x}\text{Ba}_x\text{Eu}_{0.075}\text{F}_{2.075}$ ($x = 0.00, 0.20, 0.25, 0.30, 0.35, \text{ and } 0.40$) were synthesized by precipitation from nitrate aqueous solutions using ammonium fluoride as a fluorinating agent. The lattice parameters of the samples after heat treatment at 45 °C and 600 °C increased linearly with increasing barium content. After heat treatment at 600 °C, the coherent scattering region increased from 16–

**Fig. 2.** Dependence of the lattice parameters of the $\text{Sr}_{0.925-x}\text{Ba}_x\text{Eu}_{0.075}\text{F}_{2.075}$ solid solution on the Ba content**Fig. 3.** Luminescence spectra of $\text{Sr}_{0.925-x}\text{Ba}_x\text{Eu}_{0.075}\text{F}_{2.075}$ solid solutions

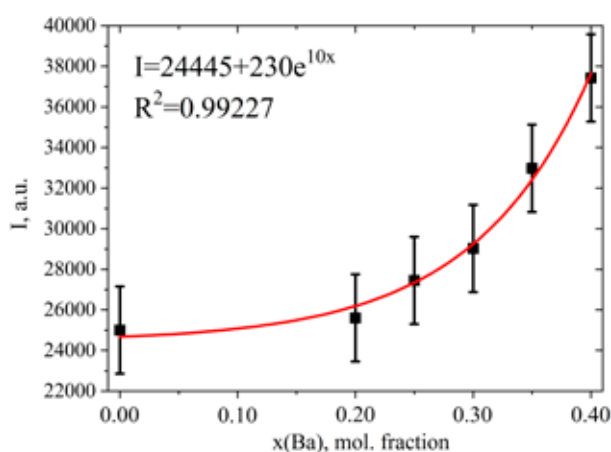


Fig. 4. Dependence of luminescence intensity of band ${}^5\text{D}_0 \rightarrow {}^7\text{F}_1$ on the barium content in the $\text{Sr}_{0.925-x}\text{Ba}_x\text{Eu}_{0.075}\text{F}_{2.075}$ solid solution

18 nm to 70–103 nm. We recorded a significant increase in the X-ray luminescence intensity of europium for ${}^5\text{D}_0 \rightarrow {}^7\text{F}_1$ with a maximum around 590 nm and ${}^5\text{D}_0 \rightarrow {}^7\text{F}_4$ with a maximum around 698 nm at constant europium concentration and increasing barium content. The intensity of the ${}^5\text{D}_0 \rightarrow {}^7\text{F}_1$ luminescence band increased with increasing barium content according to the exponential function $I = 24445 + 230e^{10x}$. Upon the increase in barium content, we observed blue and red shifts in the position of the europium luminescence bands for ${}^5\text{D}_0 \rightarrow {}^7\text{F}_1$ and ${}^5\text{D}_0 \rightarrow {}^7\text{F}_4$, respectively.

Contribution of the authors

The authors contributed equally to this article.

Conflict of interests

The authors declare that they have no known competing financial interests or personal relationships that could have influenced the work reported in this paper.

References

- Lebedev V. T., Shakhov F. M., Vul A. Y., ... Fomin E. V. X-ray excited optical luminescence of Eu in diamond crystals synthesized at high pressure high temperature. *Materials*. 2023;16: 830. <https://doi.org/10.3390/ma16020830>
- Magyar A., Hu W., Shanley T., Flatté M. E., Hu E., Aharonovich I. I. Synthesis of luminescent europium defects in diamond. *Nature Communications*. 2014;5(1): 3523. <https://doi.org/10.1038/ncomms4523>
- Yudina E. B., Aleksenskii A. E., Bogdanov S. A., ... Vul' A. Y. CVD nanocrystalline diamond film doped with Eu. *Materials*. 2022;15: 5788. <https://doi.org/10.3390/ma15165788>
- Borzdov Y. M., Khokhryakov A. F., Kupriyanov I. N., Nechaev D. V., Palyanov Y. N. Crystallization of diamond from melts of europium salts. *Crystals*. 2020;10: 376. <https://doi.org/10.3390/cryst10050376>
- Palyanov Y. N., Borzdov Y. M., Khokhryakov A. F., Kupriyanov I. N. High-pressure synthesis and characterization of diamond from europium containing systems. *Carbon*. 2021;182: 815–824. <https://doi.org/10.1016/j.carbon.2021.06.081>
- Sedov V., Kuznetsov S., Martyanov A., Ralchenko V. Luminescent diamond composites. *Functional Diamond*. 2022;2: 53–63. <https://doi.org/10.1080/26941112.2022.2071112>
- Chen H.-J., Wang X.-P., Wang L.-J., ... Liu L.-H. Bright blue electroluminescence of diamond/CeF₃ composite films. *Carbon*. 2016;109: 192–195. <https://doi.org/10.1016/j.carbon.2016.07.061>
- Chen J.-X., Wang X.-P., Wang L.-J., Yang X.-W., Yang Y. White electroluminescence of diamond/HoF₃/diamond composite film. *Journal of Luminescence*. 2020;224: 117310. <https://doi.org/10.1016/j.jlum.2020.117310>
- Sedov V. S., Kuznetsov S. V., Ralchenko V. G., ... Konov V. I. Diamond-EuF₃ nanocomposites with bright orange photoluminescence. *Diamond and Related Materials*. 2017;72: 47–52. <https://doi.org/10.1016/j.diamond.2016.12.022>
- Sedov V., Kuznetsov S., Martyanov A., ... Fedorov P. Diamond–rare earth composites with embedded NaGdF₄:Eu nanoparticles as robust photo- and X-ray-luminescent materials for radiation monitoring screens. *ACS Applied Nano Materials*. 2020;3: 1324–1331. <https://doi.org/10.1021/acsanm.9b02175>
- Sobolev B. P. *The rare earth trifluorides: the high temperature chemistry of the rare earth trifluorides. P.1. The High Temperature Chemistry of the Rare Earth Trifluorides*. Institut d'Estudis Catalans; 2000. 540 p
- Sobolev B. P. *The rare earth trifluorides. P. 2. Introduction to materials science of multicomponent metal fluoride crystals*. Institut d'Estudis Catalans, Barcelona, 2001. 520 p.
- Heise M., Scholz G., Krahl T., Kemnitz E. Luminescent properties of Eu³⁺ doped CaF₂, SrF₂, BaF₂ and PbF₂ powders prepared by high-energy ball milling. *Solid State Sciences*. 2019;91: 113–118. <https://doi.org/10.1016/j.solidstatesciences.2019.03.014>
- Peng J., Hou S., Liu X., ... Su Z. Hydrothermal synthesis and luminescence properties of hierarchical SrF₂ and SrF₂:Ln³⁺ (Ln=Er, Nd, Yb, Eu, Tb) micro/nanocomposite architectures. *Materials Research Bulletin*. 2012;47: 328–332. <https://doi.org/10.1016/j.materresbull.2011.11.030>
- Krahl T., Beer F., Relling A., Gawlitza K., Rurack K., Kemnitz E. Toward luminescent composites

by phase transfer of $\text{SrF}_2:\text{Eu}^{3+}$ nanoparticles capped with hydrophobic antenna ligands. *ChemNanoMat*. 2020;6: 1086–1095. <https://doi.org/10.1002/cnma.202000058>

16. Ermakova Y. A., Pominova D. V., Voronov V. V., ... Kuznetsov S. V. Synthesis of $\text{SrF}_2:\text{Yb}:\text{Er}$ ceramic precursor powder by co-precipitation from aqueous solution with different fluorinating media: NaF, KF and NH_4F . *Dalton Transactions*. 2022;51: 5448–5456. <https://doi.org/10.1039/D2DT00304J>

17. Kuznetsov S., Ermakova Y., Voronov V., ... Turshatov A. Up-conversion quantum yields of $\text{SrF}_2:\text{Yb}^{3+},\text{Er}^{3+}$ sub-micron particles prepared by precipitation from aqueous solution. *Journal of Materials Chemistry C*. 2018;6: 598–604. <https://doi.org/10.1039/C7TC04913G>

18. Ermakova Yu. A., Alexandrov A. A., Fedorov P. P., ... Kuznetsov S. V. Synthesis of single-phase $\text{Sr}_{1-x}\text{Ba}_x\text{F}_2$ solid solutions by co-precipitation from aqueous solutions. *Solid State Sciences*. 2022;130: 106932. <https://doi.org/10.1016/j.solidstatesciences.2022.106932>

19. Cortelletti P., Pedroni M., Boschi F., ... Spighini A. Luminescence of Eu^{3+} activated CaF_2 and SrF_2 nanoparticles: effect of the particle size and codoping with alkaline ions. *Crystal Growth & Design*. 2018;18: 686–694. <https://doi.org/10.1021/acs.cgd.7b01050>

20. Yagoub M. Y. A., Swart H. C., Noto L. L., O'Connell J. H., Lee M. E., Coetsee E. The effects of Eu-concentrations on the luminescent properties of $\text{SrF}_2:\text{Eu}$ nanophosphor. *Journal of Luminescence*. 2014;156: 150–156. <https://doi.org/10.1016/j.jlumin.2014.08.014>

21. Yuzenko K. V., Kabelitz A., Schökel A., Guilherme Buzanich A. Local structure of europium-doped luminescent strontium fluoride nanoparticles: Comparative X-ray absorption spectroscopy and diffraction study. *ChemNanoMat*. 2021;7: 1221–1229. <https://doi.org/10.1002/cnma.202100281>

22. Pan Y., Wang W., Zhou L., ... Li L. F^- - Eu^{3+} charge transfer energy and local crystal environment in Eu^{3+} doped calcium fluoride. *Ceramics International*. 2017;43: 13089–13093. <https://doi.org/10.1016/j.ceramint.2017.06.197>

23. Trojan-Piegza J., Wang Z., Kinzhybalov V., Zhou G., Wang S., Zych E. Spectroscopic reflects of structural disorder in $\text{Eu}^{3+}/\text{Pr}^{3+}$ -doped $\text{La}_{0.4}\text{Gd}_{1.6}\text{Zr}_2\text{O}_7$ transparent ceramics. *Journal of Alloys and Compounds*. 2018;769: 18–26. <https://doi.org/10.1016/j.jallcom.2018.07.233>

24. Binnemans K. Interpretation of europium(III) spectra. *Coordination Chemistry Reviews*. 2015;295: 1–45. <https://doi.org/10.1016/j.ccr.2015.02.015>

25. Drobysheva A. R., Ermakova Yu. A., Alexandrov A. A., ... Kuznetsov S. V. X-ray luminescence of $\text{SrF}_2:\text{Eu}$ nanopowders. *Optics and Spectroscopy*. 2023;131: 633. <https://doi.org/10.61011/EOS.2023.05.56516.58-22>

26. Fedorov P., Sobolev B. P. Concentration dependence of unit-cell parameters of phases $\text{M}_{1-x}\text{R}_x\text{F}_{2+x}$ with the fluorite structure. *Soviet Physics. Crystallography*. 1992;37: 651–656.

Information about the authors

Yulia A. Ermakova, Junior Researcher at the Prokhorov General Physics Institute of the Russian Academy of Sciences (Moscow, Russian Federation).

<https://orcid.org/0000-0002-9567-079X>

yulia.r89@mail.ru

Pavel P. Fedorov, Dr. Sci. (Chem.), Full Professor, Chief Researcher at the Prokhorov General Physics Institute of the Russian Academy of Sciences (Moscow, Russian Federation).

<https://orcid.org/0000-0002-2918-3926>

ppfedorov@yandex.ru

Valery V. Voronov, Cand. Sci. (Phys.–Math.), Leading Researcher at the Prokhorov General Physics Institute of the Russian Academy of Science (Moscow, Russian Federation).

<https://orcid.org/0000-0001-5029-8560>

voronov@lst.gpi.ru

Sergey Kh. Batygov, Cand. Sci. (Phys.–Math.), Leading Researcher at the Prokhorov General Physics Institute of the Russian Academy of Science (Moscow, Russian Federation).

<https://orcid.org/0000-0001-9862-0504>

sbatygov@mail.ru

Sergey V. Kuznetsov, Cand. Sci. (Chem.), Head of the Laboratory at the Prokhorov General Physics Institute of the Russian Academy of Science (Moscow, Russian Federation).

<https://orcid.org/0000-0002-7669-1106>

kouznetzovsv@gmail.com

Received 18.10.2023; approved after reviewing 31.10.2023; accepted for publication 15.11.2023; published online 25.06.2024.

Translated by Anastasiia Ananeva